ARTICLE

Thermoelasticity of MgO at High Pressures

Zi-jiang Liu[a,b], Xiao-wei Sun[c], Su-hong Ge[b], Hai-ying Wu[b], Xiu-lu Zhang[b], Xiang-dong Yang[b*]

a. Department of Physics, Lanzhou City University, Lanzhou 730070, China; b. Institute of Atomic and Molecular Physics, Sichuan University, Chengdu 610065, China; c. School of Mathematics and Physics, Lanzhou Jiaotong University, Lanzhou 730070, China

(Dated: Received on June 8, 2006; Accepted on October 18, 2006)

The thermoelastic properties of MgO over a wide range of pressure and temperature are studied using the first-principles plane wave pseudopotential method within the generalized gradient approximation. It is shown that MgO remains in the B1 (NaCl) structure at all pressures existing within the Earth, and transforms into the CsCl-type structure at 397 GPa. The athermal elastic moduli of MgO are calculated, as a function of pressure up to 150 GPa. The calculated results are in excellent agreement with experimental data at zero pressure and compare favorably with other pseudopotential predictions over the pressure regime studied. MgO is found to be highly anisotropic in its elastic properties, with the magnitude of the anisotropy first decreasing between 0 and 20 GPa and then increasing from 20 GPa to 150 GPa. The Cauchy condition is found to be strongly violated in MgO, reflecting the importance of noncentral many-body forces. The thermodynamic properties of MgO are consistent with the experimental data at ambient condition.

Key words: Thermoelasticity, High pressure, First-principles, Quasi-harmonic Debye model

I. INTRODUCTION

MgO is believed to comprise 20% of the lower mantle [1], and it is thus one of the most abundant minerals in the Earth. The thermoelasticity of MgO is important for our understanding of processes including brittle failure, flexure, and the propagation of elastic waves. However, many of its physical properties are still relatively poorly known. For example, its equation of state is relatively well known only at 298 K [2,3], while at high pressures and temperatures no experiments are reported. The elastic constants have been studied experimentally only up to 55 GPa [4]. Fiquet *et al.* also only measured several thermodynamical quantities of MgO at ambient condition [5]. Moreover, there have been no measurements of thermodynamic properties of MgO at high pressures. The B1-B2 transition has not yet been reached in experiments. A number of theoretical investigations of high pressures structure and phase stability of MgO have been done, resulting in a wide range of predicted pressures for the B1-B2 phase transition [6-13]. Correspondingly, first-principles computer simulations have been increasingly popular in exploring various properties of the Earth's materials in the geophysically relevant conditions. The full-potential linear muffin-tin-orbital (FP-LMTO) was used to study the elastic properties and their pressure dependence of four B1-type alkaline earth oxides at high pressures [14]. Recently, Oganov *et al.* used the projector augmented-wave (PAW) and pseudopotential methods to predict the thermoelasticity of MgO as a function of pressure up to 150 GPa [15].

In this work, we present first-principles predictions of the high pressure elasticity of MgO using plane-wave pseudopotential (PWPP) within the generalized gradient approximation (GGA). Our results are comparable with the previous ones at high pressures [8,15]. The thermodynamic properties of MgO at high pressures and temperatures are predicted using the quasi-harmonic Debye model.

II. METHOD

Computations are based on the density functional theory using the generalized gradient and pseudopotential approximations [16]. The soft and separable Troullier-Martins pseudopotentials [17] are used. A plane wave basis set with cutoff of 550 eV is used to expand the valence electronic wave functions such that forces and stresses are fully converged (the maximum stress is only 0.02 GPa). The Brillouin zone is sampled on a $10\times10\times10$ Monkhorst-Pack k-point mesh [18], which provides convergence of the total energy to within 1.0×10^{-6} eV/atom. The Kohn-Sham equations are solved iteratively to self-consistency within 0.5 μeV per unit cell. All the pseudopotentials are non-local. The core radii are 1.06 Å for Mg and 0.74 Å for O.

The determination of the elastic constants requires knowledge of equilibrium structure at a given pressure. We first fully optimize a single primitive cell of MgO at several pressures. The structural optimization technique uses Broydon-Fletcher-Goldfarb-Shanno [19] with variable cell shape [20]. The elastic constants are then determined from direct computation of the stresses generated by small deformations of the equilibrium unit cell. Strains of different amplitudes (-0.01-0.01) are

*Author to whom correspondence should be addressed. E-mail: liuzjscu@sohu.com, Tel: +86-28-85405526

used and the elastic constants are derived from the resulting nonlinear stress-strain relation [8]. Furthermore, we do not consider quantum corrections for zero-point energy; it is reasoned that the calculated energy of a fully optimized structure is the classical enthalpy at absolute zero, ignoring quantum effects (in particular the zero-point vibrational motion). For a structure that is sufficiently small so that its normal modes can be calculated, quantum corrections for zero-point energy and the free energy at higher temperatures can be taken into account [21].

To investigate the thermodynamic properties of MgO, we here apply the quasi-harmonic Debye model [22], in which the non-equilibrium Gibbs function $G^*(V;p,T)$ takes the following form [22]:

$$G^*(V;p,T) = E(V) + pV + A_{\rm vib}[\Theta(V);T] \quad (1)$$

where $\Theta(V)$ is the Debye temperature, and the vibrational term $A_{\rm vib}$ can be written as [23,24]

$$A_{\rm vib}(\Theta;T) = nkT\left[\frac{9}{8}\frac{\Theta}{T} + 3 \cdot \ln\left(1-e^{-\Theta/T}\right) - D\left(\frac{\Theta}{T}\right)\right] \quad (2)$$

where $D(\Theta/T)$ represents the Debye integral and n is the number of atoms per formula unit. For an isotropic solid, Θ is expressed as [23]

$$\Theta = \frac{\hbar}{k}\left(6\pi^2 V^{1/2} n\right)^{1/3} f(\sigma)\sqrt{\frac{B_S}{M}} \quad (3)$$

where M is the molecular mass per formula unit and B_S the adiabatic bulk modulus, which can be approximated by the static compressibility [22]

$$B_S \simeq B(V) = V\frac{{\rm d}^2E(V)}{{\rm d}V^2} \quad (4)$$

here the Poisson ratio σ is taken as 0.25 [25] and $f(\sigma)$ is given in Refs.[26,27]. Therefore, the non-equilibrium Gibbs function $G^*(V;p,T)$ as a function of $(V;p,T)$ can be minimized with respect to volume V as follows:

$$\left[\frac{\partial G^*(V;p,T)}{\partial V}\right]_{P,T} = 0 \quad (5)$$

By solving Eq.(5) we obtain the thermal EOS. The isothermal bulk modulus B_T, the heat capacity C_V, the entropy S and the thermal expansion coefficient α are given respectively by [28]

$$B_T(p,T) = V\left[\frac{\partial^2 G^*(V;p,T)}{\partial V^2}\right]_{P,T} \quad (6)$$

$$C_V = 3nk\left[4D\left(\frac{\Theta}{T}\right) - \frac{3\Theta/T}{e^{\Theta/T}-1}\right] \quad (7)$$

$$S = nk\left[4D\left(\frac{\Theta}{T}\right) - 3\ln\left(1-e^{-\Theta/T}\right)\right] \quad (8)$$

$$\alpha = \frac{\gamma C_V}{B_T V} \quad (9)$$

where γ is the Grüneisen parameter.

III. RESULTS AND DISCUSSION

A. Static equation of state

The lattice constant, bulk modulus, and its pressure derivative are obtained by calculating the total energy and pressure for different values of the unit cell volume and by fitting the calculated data to the third-order Birch-Murnaghan equation of state (EOS) [29]. The calculated equilibrium lattice constants, bulk modulus, and their pressure derivatives are given in Table I. Errors from the numerical fitting are less than 3 GPa for the experimental bulk modulus and less than 0.2 for K_0' [32]. Our results are comparable to the previous work [8,9,15,30,31]. The pressure dependence of the volume for MgO calculated with PW91 is shown in Fig.1. It is found that the calculated equation of state of MgO is in excellent agreement with the experimental data [2,3].

TABLE I Lattice constant, unit cell volume, bulk moduli and their pressure derivatives of MgO from the calculations and measurements

Method	a_0/Å	V_0/Å^3	K_0/GPa	K_0'
GGA	4.215	74.88	157.43	4.16
GGA [15]	4.266	77.63	151.71	4.21
GGA [15]	4.237	76.05	154.18	4.14
LDA [9]	4.240	76.20	172.60	4.00
LDA [30]	4.222	75.20	159.00	4.30
LDA [8]	4.250	76.80	159.70	4.26
LDA [31]	4.167	72.40	172.00	4.09
Exp.[32]	4.212	74.70	160.20	3.99

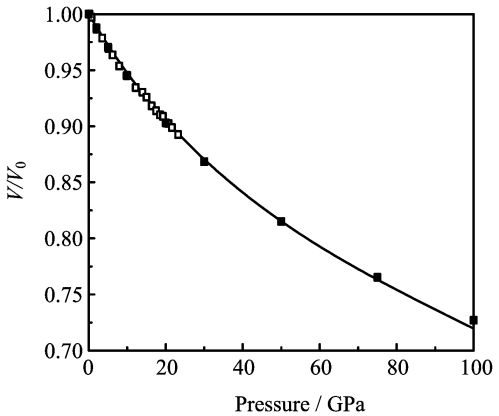

FIG. 1 Static equation of state of MgO. The solid line is the present work, the solid and open squares are the experimental data of Duffy *et al.* [2] and Fei [3] at 300 K, respectively.

ISSN 1003-7713/DOI:10.1360/cjcp2007.20(1).65.6

B. B1-B2 phase transition

We calculate the enthalpy of the two-ion primitive cell of MgO in both the B1 (NaCl) and B2 (CsCl) structures as a function of pressure from 0 to 700 GPa (Fig.2). The thermodynamic requirement of equality of free energies at a phase boundary suggests that the B1-B2 transition pressure of MgO should occur at 397 GPa. It is shown that MgO is stable in B1 phase throughout the lower mantle pressure regime. The transition involves a decrease in volume by 5.9%, clearly suggesting its first-order character. The B1-B2 transition involves an increase of coordination number from 6 for the NaCl structure to 8 for the CsCl structure, resulting in denser packing. As the coordination increases, the nearest-neighbor (Mg-O) distances increase but the second-neighbor distances decrease to give a finite volume collapse at the transition. We have compared the predicted B1-B2 transition in MgO with previous calculations [6-13,15] in Table II. However, the transition pressure has been estimated by different calculations to range from 200 GPa to over 1000 GPa. This is partly due to the diversity of methods used and partly due to small basis sets and other limitations on the accuracy of the early calculations; the pseudopotential error can also be large. Our predicted value agrees closely with the theoretical result of Strachan *et al.* [12].

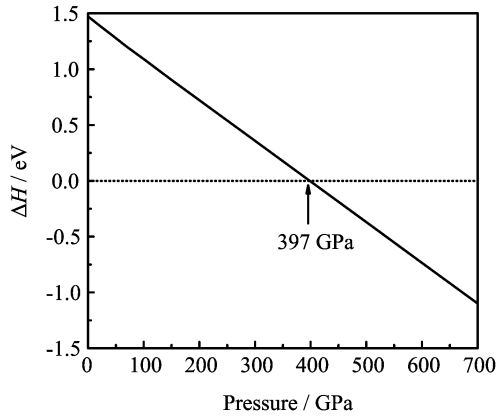

FIG. 2 The enthalpy difference between the B1 phase and B2 phase as a function of pressure.

C. Elastic moduli

The calculated athermal elastic constants at zero pressure are found to compare favorably with experiment [4] in Table III. The calculated athermal elastic constants at zero pressure are found to compare favorably with experiment [4] and previous pseudopotential calculations [15]. The small differences from experiments can be attributed to the fact that the calculations are athermal whereas experimental data are obtained at 300 K. Much of the differences between present elastic constants and the other pseudopotential results [8,33] can be accounted for. Overall, first-principles theory represents a substantial improvement on the predictions of more approximate theories, such as those based on simplified semiempirical [34] and *ab initio* models [35].

TABLE II The B1-B2 phase transition pressure of MgO

Method	$P_{\rm tr}$/GPa
GGA-ECP plane wave (this work)	397
GGA-ECP plane wave [6]	664
LDA-LCAO [7]	515
LDA-ECP plane wave [8]	451
LDA-ECP plane wave [9]	490
LDA-ECP plane wave [10]	1050
LDA-LMTO [11]	198
GGA-ECP plane wave [12]	400
LDA-LCAO [13]	512
GGA-PAW [15]	509

TABLE III Three elastic constants (C_{ij}), and bulk (K) and shear (G) moduli in GPa of MgO (B1 structure) compared with previous results at zero pressure

Method	c_{11}	c_{12}	c_{44}	K	G
PWPP	286.1	93.8	144.9	157.4	120.8
PAW[15]	279.9	90.9	142.5	153.9	120.9
PWPP[8]	291.0	90.0	137.0	157	121
PWPP[33]	323	92	152	169	135
PIB[34]	310	119	188	182	143
MEG[35]	226	142	142	170	86
Exp.[4]	297.8	95.8	154.7	163.1	130.4

The effect of pressure on the elastic constants of MgO is large, so experimental or theoretical results at ambient pressure cannot be used to reliably estimate elasticity at mantle pressures. Therefore, we predict the elastic constants of MgO. The bulk modulus of isotropic aggregate of cubic crystals is related to the elastic constant $K=(c_{11}+2c_{12})/3$. The pressure dependence of the isotropic aggregate shear modulus (G) of MgO are obtained using the Voigt-Ruses-Hill [28] averaging scheme. In Fig.3 and Fig.4, the elastic moduli of MgO are shown as functions of pressure and compared with the experimental data [4,36] and other works [8,15]. All theoretical calculations agree very well with each other and with experiments [4,36] below 20 GPa. We also find that the elastic moduli increase with increasing pressure, but with quite different slopes and curvatures.

MgO is cubic and its second-rank tensor properties are isotropic. However, elasticity, being a fourth-rank tensor property, is anisotropic even for cubic crystals, where it is conveniently expressed by the dimensionless parameter anisotropy factor $A=(2c_{44}+c_{12})/c_{11}-1$ [8]. The pressure dependence of the anisotropy factor A is

ISSN 1003-7713/DOI:10.1360/cjcp2007.20(1).65.6

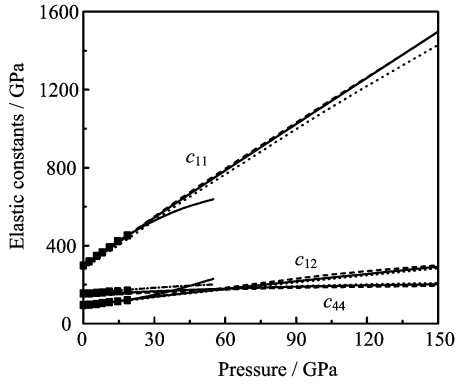

FIG. 3 Pressure dependence of elastic constants of MgO. The solid line is the present work, the dashed and dotted lines represent the calculated values of Karki *et al.* [8] and Oganov *et al.* [15] respectively. The solid squares and the dash dotted line are experimental data of Sinogeikin *et al.* [36] and Zha *et al.* [4] respectively.

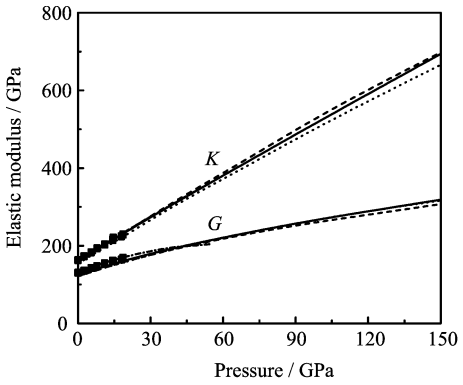

FIG. 4 Pressure dependence of bulk and shear moduli of MgO. The solid line is the present work, the dashed and dotted lines represent the calculated values of Karki *et al.* [8] and Oganov *et al.* [15] respectively. The solid squares and the dash dotted line are experimental data of Sinogeikin *et al.* [36] and Zha *et al.* [4] respectively.

shown in Fig.5. The predicted behavior of MgO is consistent with other work [8,15] and most experimental observations including those of Sinogeikin *et al.* [36], and the lower pressure data of Zha *et al.* [4]. At higher pressures, theory diverges substantially from the data of Zha *et al.* [4], who found that MgO remains essentially isotropic at pressures greater than 20 GPa. MgO turns out to be elastically highly anisotropic at ambient conditions. Anisotropy factor A decreases to zero at ∼20 GPa, changes sign, and by ∼150 GPa (which corresponds to the bottom of the Earth's mantle) adopts large negative values, making MgO probably the most elastically anisotropic mineral in the Earth's lowermost mantle. Thermal effects do not change this conclusion [37].

As shown in Fig.6, the value of Cauchy violation ($c_{12}-c_{44}-2P$) for MgO is found to be large and negative and increase in magnitude with increasing pressure.

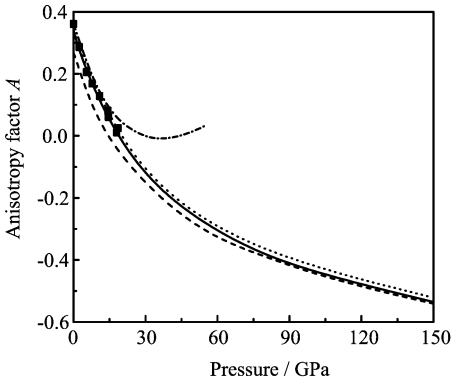

FIG. 5 Pressure dependence of anisotropy factor A of MgO. The solid line is the present work, the dashed and dotted lines represent the calculated values of Karki *et al.* [8] and Oganov *et al.* [15] respectively. The solid squares and the dash dotted line are experimental data of Sinogeikin *et al.* [36] and Zha *et al.* [4] respectively.

Our calculations almost exactly reproduce the experimental [4,36] value of Cauchy violation below ∼20 GPa. Above 20 GPa, results of Zha *et al.* [4] depart significantly from all theoretical predictions and give nonmonotonic dependences of the Cauchy deviations on pressure. The strong violation of the Cauchy conditions in MgO requires an important contribution from noncentral (many-body) forces that increases with pressure. The potential-induced breathing model appears to capture the essential physics, as this simplified model predicts correctly the Cauchy violation in the alkaline Earth oxides [38,39]. The relevant many-body force arises from a spherically symmetric breathing of the oxygen ion in response to strain-induced variations in the Madelung potential at the oxygen site.

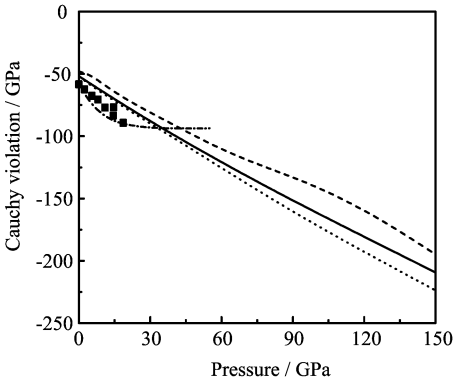

FIG. 6 Pressure dependence of Cauchy violation of MgO. The solid line is the present work, the dashed and dotted lines represent the calculated values of Karki *et al.* [8] and Oganov *et al.* [15] respectively. The solid squares and the dash dotted line are experimental data of Sinogeikin *et al.* [36] and Zha *et al.* [4] respectively.

ISSN 1003-7713/DOI:10.1360/cjcp2007.20(1).65.6

D. Thermodynamic properties

Figure 7 shows the calculated and experimental [40,41] thermal expansion (α) of MgO. One can see that the neglect of intrinsic anharmonicity in the quasi-harmonic approximation leads to an overestimation of thermal expansion, rather spectacularly at zero pressure. The calculated value compares well with the average value between 300 and 3300 K in the pressure range of 169 to 196 GPa obtained from shock-wave experiments [41]. α is found to increase strongly at lower temperatures and rapidly flatten on increasing temperature. With increasing pressure, α decreases rapidly and the effects of temperature become less and less pronounced resulting in linear high temperature behavior. It is shown that α converges to a constant value at high temperatures and pressures.

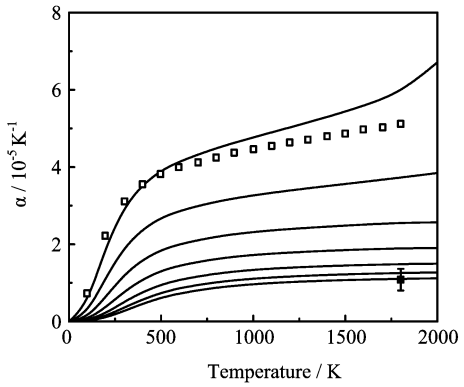

FIG. 7 Pressure and temperature dependence of thermal expansivity of MgO. The isobars at 0, 10, 30, 60, 100, 150 and 200 GPa are represented by solid lines from top to bottom. The open squares and the solid square are the experimental data of Touloukian *et al.* [40] and Duffy *et al.* [41] respectively.

The calculated heat capacity (C_V) is 36.39 J/(mol K) at ambient condition, which matches the experimental value to within 2%. As is shown in Fig.7, we arrived at values of C_V practically identical to the experimental data [42] at ambient condition. Figure 7 also illustrates that the anharmonic effects are suppressed at high pressures and C_V is very close to the Dulong-Petit limit at high pressures and temperatures. Unlike α and C_V, the high temperature dependence of entropy (S) is nearly insensitive to pressure (Fig.9).

IV. CONCLUSION

First-principles plane wave pseudopotential calculations are performed for the analysis of the structural properties of MgO under high pressure conditions. The predicted B1-B2 transition pressure of MgO is 397 GPa, which coincides with the theoretical value of Strachan *et al.* [12]. It is shown that MgO remains in the B1 ("NaCl") structure at all pressures existing within the Earth. The calculated elastic moduli of MgO up to 150 GPa are in excellent agreement with existing ambient pressure experimental data [4,36] and high pressure results from previous calculations [8,15]. We use our elastic constants to make investigations of the elastic wave velocity anisotropy for the single crystal of MgO. It exhibits strong anisotropy throughout the lower mantle and the nature of anisotropy changes significantly with depth. The predicted heat capacity and entropy are in agreement with the experimental data at ambient condition. The thermal expansion and heat capacity are shown to converge to a nearly constant value at high pressures and temperatures. Unlike α and C_V, S is nearly insensitive to pressure.

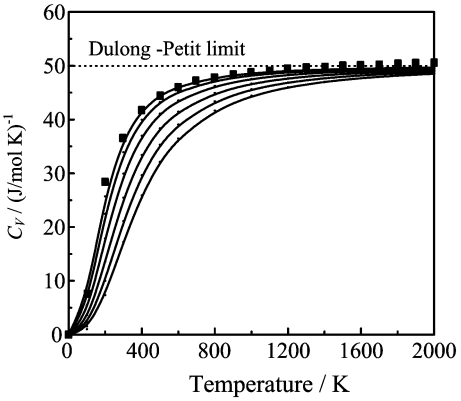

FIG. 8 Pressure and temperature dependence of heat capacity of MgO. The isobars at 0, 10, 30, 60, 100, and 150 GPa are represented by solid lines from top to bottom. The solid squares are the experimental data of Chase [42].

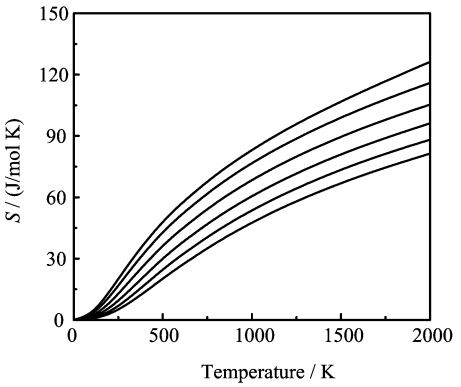

FIG. 9 Pressure and temperature dependence of entropy of MgO. The isobars at 0, 10, 30, 60, 100, and 150 GPa are represented by solid lines from top to bottom.

V. ACKNOWLEDGMENTS

This work was supported by the National Natural Science Foundation of China (No.10574096), the Specialized Research Fund for the Doctoral Program of

Higher Education of China (No.20050610010), the Natural Science Foundation of Gansu Province of China (No.3ZS051-A25-027), the Scientific Research Foundation of Education Bureau of Gansu Province of China (No.0410-01), and the 'Qing Lan' Talent Engineering Funds by Lanzhou Jiaotong University (No.QL-06-22A).

[1] G. Fiquet, Z. Krist. **216**, 248 (2001).
[2] T. S. Duffy, R. J. Hemley and H. K. Mao, Phys. Rev. Lett. **74**, 1371 (1995).
[3] Y. Fei, Am. Mineral. **84**, 272 (1999).
[4] C. S. Zha, H. K. Mao and R. J. Hemley, Proc. Natl. Acad. Sci. USA **97**, 13494 (2000).
[5] G. Fiquet, P. Richet and G. Montagnac, Phys. Chem. Miner. **27**, 103 (1999).
[6] S. Ghose, M. Krisch, A. R. Oganov, A. Beraud, A. Bosak, R. Gulve, R. Seelaboyina, H. Yang and S. K. Saxena, Phys. Rev. Lett. **96**, 035507 (2006).
[7] J. E. Jaffe, J. A. Snyder, Z. Lin and A. C. Hess, Phys. Rev. B **62**, 1660 (2000).
[8] B. B. Karki, L. Stixrude, S. J. Clark, M. C. Warren, G. J. Ackland and J. Crain, Am. Mineral **82**, 51 (1997).
[9] A. R. Oganov, M. J. Gillan and G. D. Price, J. Chem. Phys. **118**, 10174 (2003).
[10] K. J. Chang and M. L. Cohen, Phys. Rev. B **30**, 4774 (1984).
[11] G. Kalpana, B. Palanivel and M. Rajagopalan, Phys. Rev. B **52**, 4 (1995).
[12] A. Strachan, T. C. Çağin and W. A. Goddard III, Phys. Rev. B **60**, 15 084 (1999).
[13] M. P. Habas, R. Dovesi and A. Lichanot, J. Phys.: Condens. Matter **10**, 6897 (1998).
[14] T. Tsuchiya and K. Kawamura, J. Chem. Phys. **114**, 10086 (2001).
[15] A. R. Oganov and P. I. Dorogokupets, Phys. Rev. B **67**, 224110 (2003).
[16] M. C. Payne, M. P. Teter, D. C. Allan, T. A. Arias and J. D. Joannopolous, Rev. Mod. Phys. **64** 1045 (1992).
[17] N. Troullier and J. L. Martins, Phys. Rev. B **43**, 1993 (1991).
[18] H. J. Monkhorst and J. D. Pack, Phys. Rev. B **13**, 5188 (1976).
[19] T. H. Fischer and J. Almlof, J. Phys. Chem. **96**, 9768 (1992).
[20] R. M. Wentzcovitch, J. L. Martins and G. D. Price, Phys. Rev. Lett. **70**, 3947 (1993).
[21] A. T. Hagler, P. S. Stern, R. Sharon, J. M. Becker and F. Naider, J. Am. Chem. Soc. **101**, 6842 (1979).
[22] M. A. Blanco, E. Francisco and V. Luaña, Comput. Phys. Commun. **158**, 57 (2004).
[23] M. A. Blanco, A. Martín Pendás, E. Francisco, J. M. Recio and R. Franco, J. Molec. Struct. Theochem. **368**, 245 (1996).
[24] M. Flórez, J. M. Recio, E. Francisco, M. A. Blanco and A. Martn Pends, Phys. Rev. B **66**, 144112 (2002).
[25] J. P. Poirier, *Introduction to the Physics of the Earth's Interior*, Oxford: Cambridge University Press, 39 (2000).
[26] E. Francisco, J. M. Recio, M. A. Blanco and A. Martn Pendás, J. Phys. Chem. **102**, 1595 (1998).
[27] E. Francisco, G. Sanjurjo and M. A. Blanco, Phys. Rev. B **63**, 094107 (2001).
[28] R. Hill, Proc. Phys. Soc. Lond. A **65**, 349 (1952).
[29] F. Birch, J. Geophys. Res. **83**, 1257 (1978).
[30] B. B. Karki, R. M. Wentzcovitch, S. de Gironcoli and S. Baroni, Phys. Rev. B **61**, 8793 (2000).
[31] M. J. Mehl, R. E. Cohen and H. Krakauer, J. Geophys. Res. **93**, 8009 (1988).
[32] S. Speziale, C. S. Zha, T. S. Duffy, R. J. Hemley and H. K. Mao, J. Geophys. Res. **106**, 515 (2001).
[33] B. B. Karki, R. M. Wentzcovitch, S. de Gironcoli and S. Baroni, Science **286**, 1705 (1999).
[34] D. G. Isaak, R. E. Cohen and M. E. Mehl, J. Geophys. Res. **95**, 7055 (1990).
[35] A. J. Cohen and R. J. Gordon, Phys. Rev. B **14**, 4593 (1976).
[36] S. V. Sinogeikin and J. D. Bass, Phys. Earth Planet. Inter. **120**, 43 (2000).
[37] B. B. Karki, R. M. Wentzcovitch, S. de Gironcoli and S. Baroni, Science **286**, 1705 (1999).
[38] D. G. Isaak, R. E. Cohen and M. E. Mehl, J. Geophys. Res. **95**, 7055 (1990).
[39] M. J. Mehl, R. J. Hemley and L. L. Boyer, Phys. Rev. B **33**, 8685 (1986).
[40] Y. S. Touloukian, R. K. Kirdby, R. E. Taylor and T. Y. R. Lee, *Thermophysical Properties of Matter*, New York: Plenum Press, 13 (1977).
[41] T. S. Duffy and T. Ahrens, Geophys. Res. Lett. **20**, 1103 (1993).
[42] D. G. Isaak, O. L. Anderson and T. Goto, Phys. Chem. Miner. **16**, 704 (1989).

ISSN 1003-7713/DOI:10.1360/cjcp2007.20(1).65.6